Laser heterodyne spectroscopy of $^{127}I_2$ hyperfine structure near 532 nm

Ady Arie* and Robert L. Byer

Edward L. Ginzton Laboratory, Stanford University, Stanford, California 94305

Received December 30, 1992; revised manuscript received April 21, 1993

Two frequency-doubled diode-pumped Nd:YAG lasers are used to study the hyperfine spectrum of $^{127}I_2$ near 532 nm by heterodyne spectroscopy. Eight rovibrational transitions between the lowest vibrational level in the ground (X) state to vibrational levels 32–36 in the B state are observed. The measured frequency splittings are used to determine the difference in the hyperfine constants for these transitions. The standard deviation of the theoretical fit to the measured spectra is better than 10 kHz. The root Allan variance of the beat frequency between the I_2-locked lasers follows a $1.1 \times 10^{-12}/\sqrt{\tau}$ dependence for measurements times $\tau > 0.002$ s and reaches a minimum value of 2.5×10^{-13} (two-sample beat frequency of 70 Hz) at $\tau = 32$ s. A method for accurately determining the absolute frequency of the iodine lines near 532 nm is proposed.

1. INTRODUCTION

The B–X transitions of molecular iodine have been the subject of many spectroscopic measurements, resulting in a thoroughly characterized spectrum in the visible[1] and precise rotational and vibrational molecular constants.[2] The saturated absorption lines of iodine provide a relatively narrow and convenient optical frequency reference and have been used to stabilize absolutely the frequency of several gas lasers: helium–neon, argon ion, etc.[3] Four out of the five recommended wavelengths for the realization of the meter[4] correspond to hyperfine transitions in $^{127}I_2$ that coincide with laser lines.

Several frequency-doubled Nd:YAG laser systems have been used to study the hyperfine spectrum of iodine near 532 nm. Kruzhalov *et al.*[5] used an intracavity-doubled Nd:YAG laser and also locked the laser frequency to hyperfine transitions, whereas external doubling of a pulsed-injection-seeded laser was used by Esherick and Owyoung[6] for fluorescence excitation and Doppler-free spectroscopy of iodine. Recently we absolutely stabilized the frequency of resonantly externally doubled diode-pumped Nd:YAG lasers to 2.3 parts in 10^{12} by locking to iodine hyperfine transitions.[7]

The narrow linewidths and relatively wide tuning range of the monolithic diode-laser-pumped Nd:YAG lasers that are doubled into the visible provide an excellent tool for investigating the iodine hyperfine transitions. In this paper we use the ability to lock the second harmonic of two lasers to iodine hyperfine transitions to measure precisely the hyperfine frequency splitting of several rovibrational lines that fall within the tuning range of the doubled laser by heterodyne spectroscopy. These results are then used to determine the hyperfine constants of the measured transitions.

The experimental setup and the frequency-stability measurements are described in Section 2. Section 3 contains the frequency splitting, spectra, and hyperfine constants of the investigated lines. In Section 4 we discuss the results and propose a method for accurately measuring the frequency of the iodine transitions near 532 nm.

2. EXPERIMENTAL RESULTS

The experimental setup is shown in Fig. 1. We used two Lightwave Electronics Model 122 Nd:YAG monolithic diode laser-pumped nonplanar ring lasers, emitting 300 mW at 1064 nm. Each laser frequency was externally doubled with a MgO:$LiNbO_3$ monolithic crystal resonator, heated to its phase-matching temperature (~108 °C). To provide high conversion efficiency with a fixed output power, the doubling crystal resonator was frequency locked to the Nd:YAG pump frequency by a servo that controlled the $LiNbO_3$ resonator temperature.[7] The 532-nm output of the doubler was the source for FM Doppler-free saturation spectroscopy of iodine.

The modulation frequencies of the electro-optic modulators were 10 and 10.9 MHz. For the frequency-splitting measurements we replaced the 10-MHz modulator by a 4-MHz $LiTaO_3$ modulator, since several pairs of iodine hyperfine lines were found to be nearly 10 MHz apart. We acousto-optically shifted the pump beam to prevent interferometric noise problems between the reflected pump and the probe.[8] We used 10- and 15-cm-long $^{127}I_2$ cells.[9] These cells were made of quartz, and the cold finger of each cell was held at a temperature of 0 °C. For the heterodyne splitting measurements the 10-cm cell was replaced by a calibrated 8.5-cm cell.[10] This cell was tested at 633 nm by a beat-frequency measurement against an iodine-stabilized reference helium–neon laser (BIPM4): the average frequency shift of four hyperfine transitions of the $R(127)11$–5 line was less than 2.5 kHz.[10] The optical beam inside the cell was elliptic, having a ~1 mm × 2 mm diameter (transit-time broadening <40 kHz). The half-wave plate and polarizing beam splitter were adjusted to maximize the pump power reflected from the polarizing beam splitter into the iodine cell while maximizing the transmitted power of the orthogonally polarized probe beam through the polarizing beam splitter to the detector. Under these conditions the measured full width at half-maximum linewidth was 1.3 MHz. The dispersion signal of a hyperfine line could be fed back into the piezoelectric transducer frequency actuator of the laser through a servo

0740-3224/93/111990-08$06.00

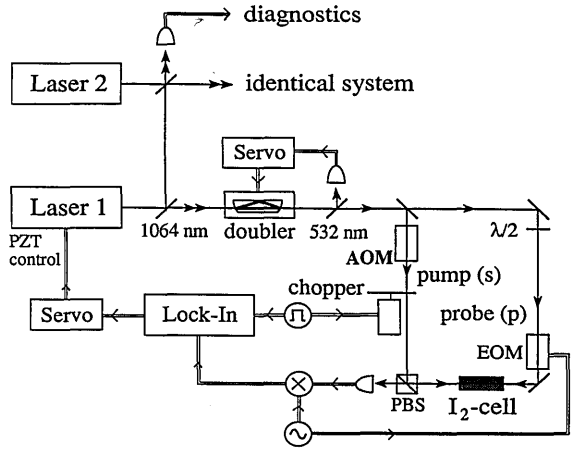

Fig. 1. Experimental setup. AOM, acousto-optic modulator; EOM, electro-optic modulator; PBS, polarizing beam splitter; PZT, piezoelectric transducer. The cold finger of each iodine cell was held at a temperature of 0 °C.

Table 1. $^{127}I_2$ Absorption Lines within the Tuning Range of the Frequency-Doubled Nd:YAG Laser

Line	Measured (cm^{-1})[a]	Calculated (cm^{-1})[b]	Assignment
1106	18 787.1285	18 787.1270	$P(119)35-0$
1107	18 787.2800	18 787.2792	$R(86)33-0$
1108	18 787.3389	18 787.3378	$R(106)34-0$
1109	18 787.8042	18 787.7807	$R(134)36-0$
		18 787.8008	$P(83)33-0$
1110	18 788.3371	18 788.3345	$R(56)32-0$
1111	18 788.4454	18 788.4345	$P(103)34-0$
		18 788.4417	$P(53)32-0$

[a]Ref. 1.
[b]Ref. 2.

controller, thereby locking the laser frequency to the hyperfine line of the iodine. We have observed eight relatively strong rovibrational transitions within the tuning range of the doubled laser (18 787–18 789 cm^{-1}). Using vibrational bandhead energies and rotational constants,[2] we have assigned the vibrational and rotational numbers for these lines; see Table 1. The line numbers and measured frequencies are taken from Ref. 1. Note that lines 1109 and 1111 each contain two rovibrational transitions. Several additional transitions between the 1 and 2 vibrational levels in the X state to vibrational levels 35–42 in the B state fall within the tuning range of the laser. We observed the hyperfine structure of some of them, but detailed measurements were made only on the strong iodine lines (Table 1), originating from the lowest vibrational level in the X state.

Two completely independent systems have been built, with each laser frequency doubled and locked to its own iodine cell. The heterodyne beat-note signal between the lasers is measured at 1064 nm by use of a photodetector followed by a frequency analyzer. The stability of the locked lasers is calculated with the Allan variance

$$\sigma^2(\tau) = \frac{1}{2\nu^2(M-1)} \sum_{i=1}^{M-1} (y_{i+1} - y_i)^2, \qquad (1)$$

where τ is the time between successive measurements as well as the duration of each frequency measurement, ν is the mean optical frequency (281.63 THz at 1064 nm), M is the number of measurements, and y_i is the ith frequency measurement. Figure 2 shows the root Allan variance as a function of τ when both lasers are locked to the a_1 line of $R(56)32-0$ (we use the modern notation in which a_i denotes the ith hyperfine line in an increasing frequency order). We used different modulation frequencies for the acousto-optic frequency shifters of the two systems; hence the center beat frequency was 23.3 MHz, although both lasers were locked to the same hyperfine line in each cell. For $\tau > 0.002$ s the root Allan variance can be represented in a compact form as $1.1 \times 10^{-12}/\sqrt{\tau}$, and the actual measurement results differ by less than 40% from this dependence. The lowest value of 2.5×10^{-13} (frequency deviation of 70 Hz) is reached at $\tau = 32$ s. This represents an order-of-magnitude improvement in the stability with respect to our previous results.[7] The main improvements in the experimental system are due to cooling and temperature stabilizing the iodine cells, eliminating the interferometric noise between the scattered pump and probe by acousto-optic shift of the pump beam, and defocusing the beams to reduce the power broadening. Similar levels of stability were obtained with locking to other isolated hyperfine transitions. Figure 3 shows the time variation of the beat frequency between the two

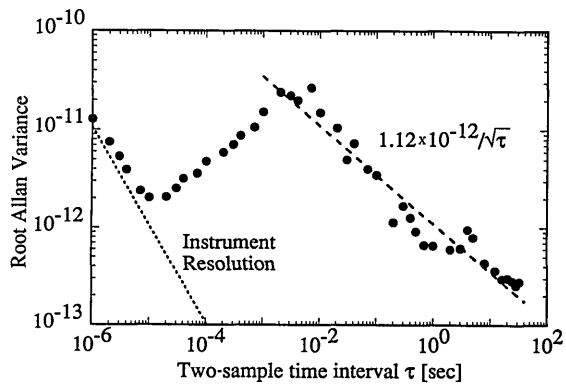

Fig. 2. Root Allan variance between two lasers locked to the a_1 line of $R(56)32-0$. $M = 100$, $\nu = 281.63$ THz. The minimum value of 2.5×10^{-13} is reached at $\tau = 32$ s and corresponds to a frequency deviation of 70 Hz.

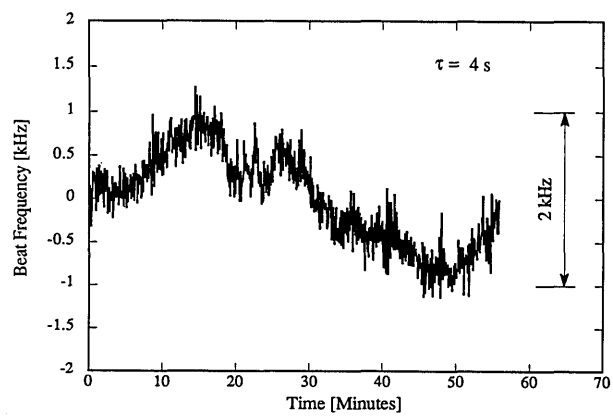

Fig. 3. Time variation of the beat frequency at 1064 nm (around a center frequency of 23.3 MHz) between two frequency-doubled iodine-locked Nd:YAG lasers measured over a 1-h period.

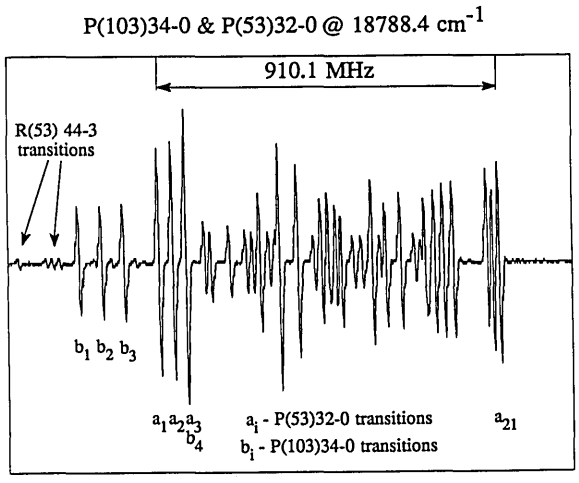

Fig. 4. FM saturated absorption spectrum of $P(53)32-0$ and $P(103)34-0$. The weak lines near the b_1 line of $P(103)34-0$ belong to the $R(53)44-3$ transition. Laser temperature, ~30.5 °C.

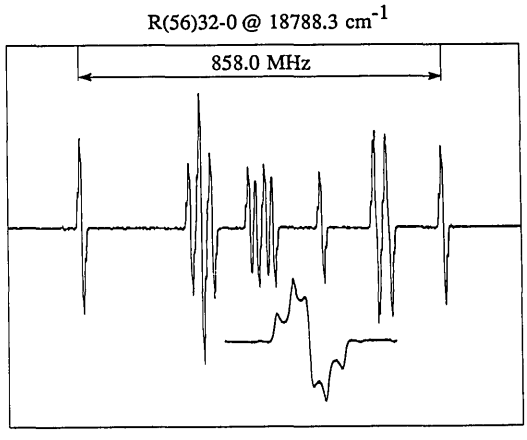

Fig. 5. FM saturated absorption spectrum of $R(56)32-0$. The inset is an expanded scan of the a_1 line. The difference between the two side peaks is approximately 21.8 MHz (twice the modulation frequency of the electro-optic modulator). Laser temperature, ~31 °C.

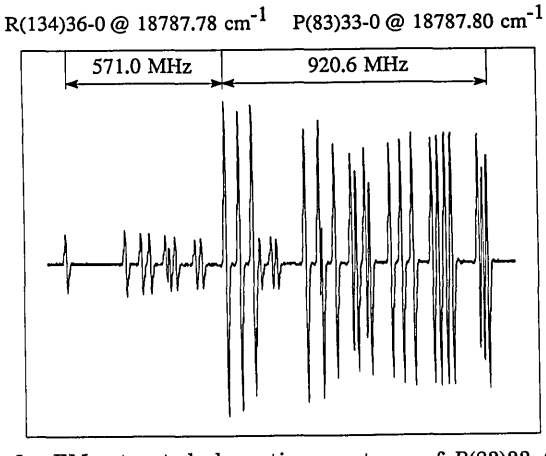

Fig. 6. FM saturated absorption spectrum of $P(83)33-0$ and $R(134)36-0$. Laser temperature, ~39 °C.

iodine-locked lasers over a 1-h period. The maximim frequency excursion in this measurement is approximately 2 kHz. We believe that on this time scale pressure-induced line shifts (~1 MHz/Torr, Ref. 11) that are due to temperature variation of the iodine-cell cold finger are the main cause for these frequency excursions.

The FM saturated absorption spectra of the iodine lines, shown in Figs. 4–9, were obtained with the servo controller turned off and a ramp voltage applied to the temperature frequency actuator of the laser. The center temperature in which the Nd:YAG laser was operated for each of these lines is listed in the figure captions. In these measurements we used the 15-cm-long iodine cell, with its cold

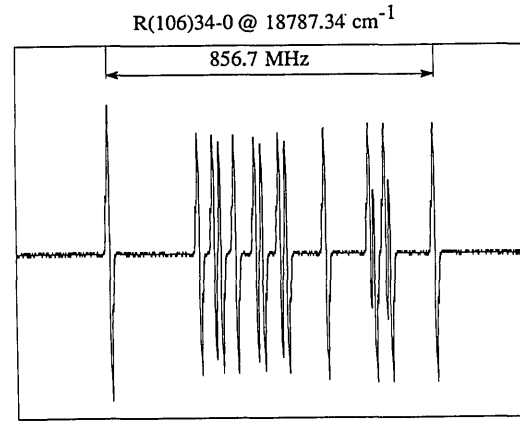

Fig. 7. FM saturated absorption spectrum of $R(106)34-0$. Laser temperature, ~44 °C.

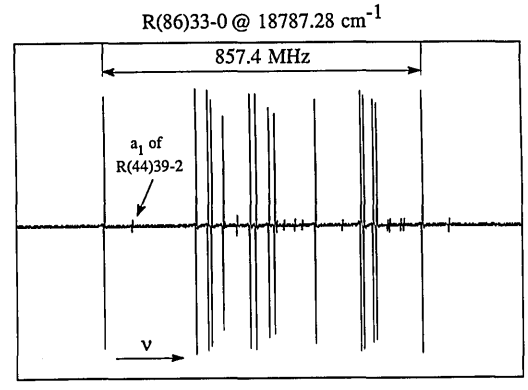

Fig. 8. FM saturated absorption spectrum of $R(86)35-0$. The weak lines in this spectrum belong to the $R(44)39-2$ line. Laser temperature, ~44.5 °C. The improved resolution is due to the lower (4-MHz) modulation frequency.

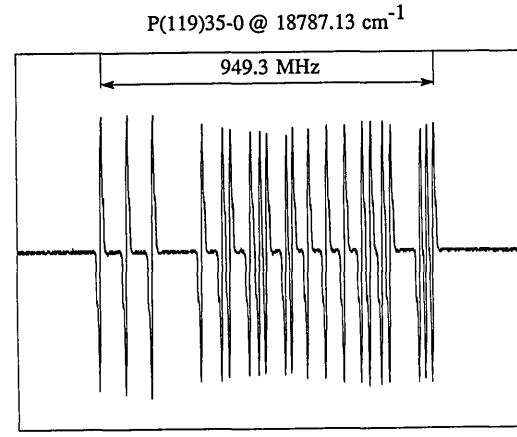

Fig. 9. FM saturated absorption spectrum of $P(119)35-0$. Laser temperature, ~45.5 °C.

Table 2. Frequency Spacing (MHz) between Rovibrational Transitions

Line	a_1 Spacing[a]	Line-Center Spacing[b]	Calculated[c]	Δ
$P(119)35-0$	−36 268.4	−36 194.9[d]	−36 199.9	−5.04
$R(86)33-0$	−31 618.8	−31 619.1	−31 637.1	−17.97
$R(106)34-0$	−29 863.1	−29 863.8	−29 880.3	−16.49
$R(134)36-0$	−16 602.1		−16 602.5	
$P(83)33-0$	−16 031.1	−15 983.4	−15 999.9	−16.55
$R(56)32-0$	0	0	0	0
$P(103)34-0$	2 956.0		2 997.9	
$P(53)32-0$	3 171.2 (±0.2 MHz)	3 207.4	3 213.8 (±112 MHz)	6.41

[a]Beat frequency between the a_1 line of each rovibrational transition and the a_1 line of $R(56)32-0$.
[b]Calculated using expressions (2a) and (2b) and the measurements of the a_1 spacings.
[c]Difference between calculated absolute frequencies (see third column in Table 1).
[d]The measured a_1-a_{21} beat frequency of $P(119)35-0$ is 949.286 MHz.

finger held at a temperature of 0 °C. The number of observed transitions (15 or 21) is in agreement with the selection rules for rotational number transition from the X to the B state. It is easily seen that lines 1109 and 1111 (Figs. 4 and 6) each contain two rovibrational transitions. A careful examination of line 1107 (Fig. 8) reveals some weak lines, which belong to the $R(44)39-2$ transition, with a calculated center frequency[2] for 18 787.2803 cm^{-1}. In Fig. 4 one can also observe the high-frequency components of the $R(53)44-3$ transition, with a calculated center frequency of 18 788.3859 cm^{-1} near the b_1 line of $P(103)34-0$. In Figs. 4–7 and 9 the dark spots in the middle of the positive and the negative slopes of each of the hyperfine signals are the 10.5-MHz FM side peaks. These side peaks are clearly observed on an expanded scan of the a_1 line of $R(56)32-0$; see the inset in Fig. 5. To demonstrate the improved resolution at lower modulation frequencies, we obtained Fig. 8 with a modulation frequency of 4 MHz.

We have locked one of the lasers to an isolated hyperfine component to measure the hyperfine frequency splitting. This laser served as a frequency reference, while the second laser was locked in succession to different hyperfine components of the calibrated iodine cell, and we measured the beat frequency by taking the average of 30 successive 4-s frequency measurements. The analysis of the hyperfine frequency splitting measurements is carried out in Section 3.

We have also measured the frequency spacing between the Doppler-broadened lines. This was done by locking one laser to the a_1 line of $R(56)32-0$ while locking the second laser to the a_1 line of each of the other rovibrational transitions. The beat frequency at 1064 nm was measured with the HP71400C light-wave signal analyzer (bandwidth 22 GHz). It was shown[12] that the center of an unblended Doppler-broadened line can be approximately estimated from the position of the hyperfine lines: for a 15-component transition, the center is given by

$$f(a_1) + 5[f(a_{15}) - f(a_1)]/9, \tag{2a}$$

whereas for a 21-component transition it is

$$f(a_2) + 5[f(a_{20}) - f(a_2)]/9. \tag{2b}$$

Using these formulas and the measured frequency spacings of the a_1 lines, we can calculate the frequency spacing between the centers of the Doppler-broadened lines. These results can be compared with the difference between the absolute frequencies of the iodine lines, calculated using the molecular constants,[2] as shown in Table 2. It is encouraging to find that, although the accuracy of the absolute frequency prediction using molecular constants is only 2 parts in 10^7 (112 MHz),[12] the agreement with our measurements in this range is much better.

3. DETERMINING HYPERFINE CONSTANTS

We used the measured iodine spectra to determine the hyperfine constants for these transitions. We follow the procedure outlined by Foth and Spieweck[13]: the Hamiltonian of the hyperfine interactions can be written as

$$H_{hfs} = H_{EQ} + H_{SR} + H_{SSS} + H_{TSS}, \tag{3}$$

where $H_{EQ}(eQq)$, $H_{SR}(C)$, $H_{SSS}(a)$, $H_{TSS}(d)$ represent the electric quadrupole, spin–rotation, scalar spin–spin, and tensor spin–spin interactions, respectively, and the symbols in parentheses denote the constants of each of these interactions. For the electric quadrupole interactions we have also considered rotational levels separated by ±2, where the rotational energy spacings were taken from Ref. 2. The frequency splitting depends strongly on the difference in the hyperfine constants between the B and the X states, but exhibits only weak dependence on the absolute values of these constants. We have therefore used fixed values for the constants of the X state, based on the measurements of the $v'' = 0$, $J'' = 13$ level,[14] while fitting the parameters of the B level to the experimental measurements (v'' and J'', respectively, denote the vibrational and rotational numbers in the X state).

We performed the fitting by minimizing the standard deviation,[15]

$$\sigma = \left[\frac{1}{N-4}\sum (x_i - y_i)^2\right]^{1/2}, \tag{4a}$$

where N is the number of measured lines and x_i and y_i are the measured and the fitted values, respectively. Once the minimum standard deviation was reached, the standard deviation for each of the four hyperfine constants was calculated[15]:

$$\sigma_z = \sigma\left[\sum\left(\frac{\partial z}{\partial y_i}\right)^2\right]^{1/2}, \tag{4b}$$

where z denotes each of the four constants.

Our first set of measurements was made with modulation frequencies of 10 and 10.9 MHz. However, the hyperfine spectrum of the lines that we investigated included several pairs of lines that are ~10 MHz apart [e.g., the $a_{11}-a_{12}$, $a_{13}-a_{14}$ lines of $R(86)33-0$ and $R(106)34-0$]. This resulted in a shift of the measured frequencies for these lines, owing to the interaction of the FM sideband with the neighboring line. The largest deviations (more than 100 kHz) between the theoretical fit and the experimental measurements were obtained in these cases. Hence we replaced the 10-MHz $LiNbO_3$ modulator with a 4-MHz $LiTaO_3$ modulator. The reduction in modulation frequency led to a substantial improvement in the measured

Table 3. Measured and Calculated Hyperfine Components of $P(53)32\text{–}0$[a]

	Measured (MHz)	Calculated (MHz)	Calc − Meas (MHz)	$F-J$	I
a_1	0	0	0	−5	5
a_2	37.530	37.529	−0.001	0	1
a_3	72.812[b]	73.072		5	5
a_4	271.341	271.341	0.0005	−4	5
a_5		322.350		1	3
a_6		324.449		−1	3
a_7		373.187		4	5
a_8		436.904		−3	5
a_9		455.282		−2	3
a_{10}		476.320		2	3
a_{11}		489.952		3	3
a_{12}		572.453		−3	3
a_{13}	609.054	609.060	0.006	0	3
a_{14}	648.974	648.984	0.010	3	5
a_{15}		712.953		−2	5
a_{16}	739.285	739.286	0.002	−1	5
a_{17}		762.634		1	5
a_{18}	788.448	788.443	−0.005	2	5
a_{19}	879.126	879.119	−0.007	−1	1
a_{20}	892.968	892.964	−0.005	0	5
a_{21}	910.110	910.106	−0.004	1	1

[a]Fitting parameters are $\Delta eQq = 1908.4757 \pm 0.08$ MHz, $\Delta C = 86.047 \pm 0.15$ kHz, $\Delta a = -10.27 \pm 4.4$ kHz, and $\Delta d = -44.4 \pm 3.7$ kHz, and the standard deviation of the fit is 6.51 kHz. Reference line is a_1.
[b]Unresolved from the b_4 line of $P(103)34\text{–}0$, hence not used in the fitting process.

Table 4. Measured and Calculated Hyperfine Components of $R(56)32\text{–}0$[a]

	Measured (MHz)	Calculated (MHz)	Calc − Meas (MHz)	$F-J$	I
a_1	0	0	0	0	2
a_2	259.698	259.695	−0.002	−4	4
a_3		285.511		1	2
	285.862[b]				
a_4		286.220		−1	2
a_5	311.360	311.360	−0.0002	4	4
a_6	401.480	401.481	0.001	−3	4
a_7	416.998	416.998	−0.001	−2	4
a_8	439.626	439.628	0.002	2	4
a_9	455.341	455.342	0.001	3	4
a_{10}	571.548	571.546	−0.002	0	4
a_{11}	698.045	698.059	0.014[c]	−2	2
a_{12}	702.774	702.759	−0.014[c]	−1	4
a_{13}	726.031	726.035	0.003	1	4
a_{14}	732.211	732.209	−0.002	2	2
a_{15}	857.960	857.959	−0.001	0	0

[a]Fitting parameters are $\Delta eQq = 1908.4057 \pm 0.01$ MHz, $\Delta C = 86.34 \pm 0.23$ kHz, $\Delta a = -10.60 \pm 5.4$ kHz, and $\Delta d = -44.95 \pm 4.5$ kHz, and the standard deviation of the fit is 6.92 kHz. Reference line is a_1.
[b]Unresolved lines.
[c]The a_{11} and a_{12} lines are only 4.7 MHz apart, whereas the modulation frequency is 4 MHz. This is probably causing the large deviation between measurement and theory.

accuracy for closely spaced lines, as well as to an increase in resolution. Since the reference system was locked each time to a fixed, isolated hyperfine line, the 10.9-MHz modulation frequency was left unchanged.

The difference in the hyperfine constants, as well as the measured and calculated frequency splitting, are given in Tables 3–8. $F - J$ denotes the difference between the angular momentum (F) and the rotational number in the B state (J), and I is the total nuclear spin. Only lines that could be resolved were used in the fitting process, since locking to some of the unresolved lines was not very stable. We include, however, the measurements of these unresolved lines.

The measured splitting of the $R(56)32\text{–}0$ line (Table 4) is slightly different than in our previous measurement.[7] We believe that the results of Table 4 are more accurate, since the systematic errors have been reduced and the fre-

Table 5. Measured and Calculated Hyperfine Components of $P(83)33\text{–}0$[a]

	Measured (MHz)	Calculated (MHz)	Calc − Meas (MHz)	$F-J$	I
a_1	−48.848[b]	−48.7767		−5	5
a_2	0	0	0	0	1
a_3	47.048	47.052	0.004	5	5
a_4	232.568[b]	232.558		−4	5
a_5	281.444	281.446	0.002	−1	3
a_6	289.888	289.890	0.002	1	3
a_7	337.046	337.049	0.003	4	5
a_8	395.587	395.585	−0.002	−3	5
a_9	411.720	411.724	0.004	−2	3
a_{10}	444.760	444.755	−0.006	2	3
a_{11}	458.760	458.754	−0.006	3	3
a_{12}	532.457	532.456	−0.001	−3	3
a_{13}	571.287	571.287	−0.0004	0	3
a_{14}	611.150	611.152	0.002	3	5
a_{15}	679.287	679.292	0.006	−2	5
a_{16}	701.347	701.353	0.006	−1	5
a_{17}	726.022	726.027	0.005	1	5
a_{18}	747.344	747.347	0.004	2	5
a_{19}	841.936	841.933	−0.003	−1	1
a_{20}	855.941	855.936	−0.006	0	5
a_{21}	871.705	871.700	−0.006	1	1

[a]Fitting parameters are $\Delta eQq = 1906.9447 \pm 0.077$ MHz, $\Delta C = 94.483 \pm 0.56$ kHz, $\Delta a = -10.14 \pm 4.2$ kHz, and $\Delta d = -48.65 \pm 4.5$ kHz, and the standard deviation of the fit is 4.50 kHz. Reference line is a_2.
[b]a_1 and a_4 were measured but not used in the fitting process, since they lie close to the a_{10} and a_{15} lines of $R(134)36\text{–}0$, see Tables 2 and 6, which shifted the measured frequencies for these two lines.

Table 6. Measured and Calculated Hyperfine Components of $R(134)36\text{–}0$[a]

	Measured (MHz)	Calculated (MHz)	Calc − Meas (MHz)	$F-J$	I
a_1	0	0	0	0	2
a_2		212.275		−4	4
a_3	269.647	269.649	0.002	−1	2
a_4	300.075	300.089	0.013	1	2
a_5	356.780	356.783	0.002	4	4
a_6	369.626	369.625	−0.001	−3	4
a_7	391.664	391.674	0.009	−2	4
a_8	462.596	462.588	−0.008	2	4
a_9	484.314	484.318	0.004	3	4
a_{10}		569.776		0	4
a_{11}		674.726		−2	2
a_{12}	691.949	691.948	−0.001	−1	4
a_{13}	732.420	732.403	−0.017	1	4
a_{14}	750.452	750.458	0.006	2	2
a_{15}		855.214		0	0

[a]Fitting parameters are $\Delta eQq = 1902.2662 \pm 0.15$ MHz, $\Delta C = 128.694 \pm 1.6$ kHz, $\Delta a = -15.14 \pm 8.8$ kHz, and $\Delta d = -64.7 \pm 7$ kHz, and the standard deviation of the fit is 9.81 kHz. Reference line is a_1.

Table 7. Measured and Calculated Hyperfine Components of $R(106)34\text{–}0$[a]

	Measured (MHz)	Calculated (MHz)	Calc − Meas (MHz)	$F - J$	I
a_1	0	0	0	0	2
a_2	236.870	236.870	0.0002	−4	4
a_3	276.953	276.938	−0.015	−1	2
a_4	293.871	293.857	−0.014	1	2
a_5	333.343	333.349	0.006	4	4
a_6	387.631	387.634	0.003	−3	4
a_7	404.629	404.631	0.002	−2	4
a_8	451.167	451.169	0.002	2	4
a_9	467.977	467.979	0.002	3	4
a_{10}	570.790	570.790	0.0002	0	4
a_{11}	687.525	687.532	0.007	−2	2
a_{12}	698.652	698.654	0.002	−1	4
a_{13}	728.254	728.251	−0.003	1	4
a_{14}	740.179	470.176	−0.002	2	2
a_{15}	856.663	856.664	0.001	0	0

[a]Fitting parameters are $\Delta eQq = 1905.2577 \pm 0.125$ MHz, $\Delta C = 104.829 \pm 0.18$ kHz, $\Delta a = -9.87 \pm 5.7$ kHz, and $\Delta d = -53.67 \pm 5.4$ kHz, and the standard deviation of the fit is 7.13 kHz. Reference line is a_1.

Table 8. Measured and Calculated Hyperfine Components of $R(86)33\text{–}0$[a]

	Measured (MHz)	Calculated (MHz)	Calc − Meas (MHz)	$F - J$	I
a_1	0	0	0	0	2
a_2	248.204	248.204	0.0006	−4	4
a_3	280.800	280.799	−0.001	−1	2
a_4	290.505	290.501	−0.004	1	2
a_5	322.528	322.527	−0.001	4	4
a_6	395.382	395.384	0.002	−3	4
a_7	410.695	410.692	−0.003	−2	4
a_8	445.755	445.757	0.001	2	4
a_9	460.968	460.972	0.004	3	4
a_{10}	571.257	571.256	−0.001	0	4
a_{11}	693.196	693.197	0.0004	−2	2
a_{12}	701.367	701.369	0.002	−1	4
a_{13}	726.702	726.702	0.001	1	4
a_{14}	735.789	735.789	−0.001	2	2
a_{15}	857.376	857.375	−0.001	0	0

[a]Fitting parameters are $\Delta eQq = 1906.8107 \pm 0.044$ MHz, $\Delta C = 95.043 \pm 0.05$ kHz, $\Delta a = -10.09 \pm 1.4$ kHz, and $\Delta d = -48.54 \pm 0.7$ kHz, and the standard deviation of the fit is 2.25 kHz. Reference line is a_1.

quency stability is an order of magnitude better. We did not fit the $P(103)34\text{–}0$ and the $P(119)35\text{–}0$ transitions, since only a small number of hyperfine transitions were measured for each one of them.

The effect of the scalar and tensor spin–spin constants on the hyperfine spectrum is much weaker than that of the electric quadrupole and spin–rotation constants. This explains why the spin–spin constants were determined with a lower accuracy. The standard deviation of the fit for all measured lines was better than 10 kHz. The worst fit, with a standard deviation of 9.8 kHz, is obtained for the relatively weak $R(134)36\text{–}0$ line, in which the experimental errors were the largest.

4. DISCUSSION

The fitted hyperfine constants for the lines studied in this paper are summarized in Table 9. There are two occurrences of two transitions belonging to the same vibrational bands ($32\text{–}0, 33\text{–}0$). Three of the four hyperfine constants depend only on the vibrational number, and only ΔeQq exhibits a weak dependence on the rotational number.[16] As is seen from Table 9, the values of the hyperfine constants are indeed in good agreement for each of the two pairs. It is interesting to note that this is not the first time that hyperfine transitions in the $32\text{–}0$ band were measured: Levenson and Schawlow[17] measured the $P(10)$ and $R(13)$ pair at 530.8 nm using a krypton-ion laser. Also note that measuring the $P(103)34\text{–}0$ line will form a third pair of transitions with the same vibrational numbers.

The dependence of the ΔeQq and ΔC constants on the vibrational numbers is consistent with measurements of iodine lines at other wavelengths[17]: while only slight changes are observed in ΔeQq, ΔC increases by 50% from the $32\text{–}0$ to the $36\text{–}0$ transitions. This is because the thirty-sixth vibrational level lies closer to the dissociation limit.[17] We have compared our results for ΔeQq and ΔC with the empirical formulas of Glaser.[18] Our values for ΔeQq are higher by 1.5–2 MHz than the empirical values, whereas the values of ΔC are typically a few (less than 10) kilohertz below the empirical predictions, except for the $R(134)36\text{–}0$ line, whose measured value is 9.5 kHz above the predicted value.

An iodine-locked Nd:YAG laser offers some advantages with respect to other optical frequency standards in the visible, such as iodine-stabilized helium–neon and argon-ion lasers. The 633-nm helium–neon laser locked to the $R(127)11\text{–}5$ transition is probably the most widely used optical frequency reference in the visible. However, the population of the $v'' = 5$ level is very low near room temperature [the vibrational term of the ground state is 214.5 cm^{-1} (Ref. 19)], thus requiring a relatively long cell or multiple passes by intracavity-resonant or externally resonant absorption. Furthermore, the available power levels are in the milliwatt range. As is shown in this paper, the Nd:YAG laser can be locked to several strong absorption lines originating from the $v'' = 0$ level, and power levels exceeding 100 mW have been demonstrated.[20] The

Table 9. Standard Deviation of the Fit (σ) and Hyperfine Constants Difference

Line	σ (kHz)	ΔeQq (MHz)	ΔC (kHz)	Δa (kHz)	Δd (kHz)
$P(53)32\text{–}0$	6.51	1908.4757 ± 0.08	86.047 ± 0.15	−10.27 ± 4.4	−44.4 ± 3.7
$R(56)32\text{–}0$	6.92	1908.4057 ± 0.01	86.34 ± 0.23	−10.60 ± 5.4	−44.95 ± 4.5
$P(83)33\text{–}0$	4.50	1906.9447 ± 0.077	94.483 ± 0.56	−10.14 ± 4.2	−48.65 ± 4.5
$R(86)33\text{–}0$	2.25	1906.8107 ± 0.044	95.043 ± 0.05	−10.09 ± 1.4	−48.54 ± 0.7
$P(106)34\text{–}0$	7.13	1905.2577 ± 0.125	104.829 ± 0.18	−9.87 ± 5.7	−53.67 ± 5.4
$R(134)32\text{–}0$	9.81	1902.2662 ± 0.15	128.694 ± 1.6	−15.14 ± 8.6	−64.7 ± 7

main advantages of the monolithic Nd:YAG laser with respect to argon-ion lasers are in linewidth, size, and electrical efficiency, thus offering the possibility of a compact and portable frequency-stabilized laser system. It should also be mentioned that since both the fundamental and second-harmonic frequencies are available, it may be possible to compensate partially for dispersion effects in precise length measurements.

If a Nd:YAG laser locked to iodine hyperfine transitions is to become an optical frequency and length standard, it is important to determine accurately the absolute frequency of the iodine hyperfine transitions near 532 nm. At the moment the center frequency of the Doppler-broadened lines of iodine is known to only 2 parts in 10^7.[12] The frequencies of several iodine hyperfine transitions that match helium–neon laser lines were measured by a frequency chain that starts from the cesium atomic clock with an accuracy of several parts in 10^{10}.[21] While new methods have been recently suggested for accurate measurement of the frequency of light,[22,23] it is worth mentioning that the sum frequency of the 3.19-μm, CH_4-stabilized helium–neon laser (88.376 THz, Ref. 4) and the 0.633-μm iodine-stabilized helium–neon laser (473.612 THz, Ref. 21) lies only 1.3 THz below the iodine transitions that were studied in this paper. Three-orders-of-magnitude improvement in the accuracy of the absolute frequency of these transitions may be achieved with these two helium–neon lasers. For example, difference frequency mixing between the iodine-stabilized Nd:YAG and the CH_4-stabilized helium–neon lasers will generate red light whose frequency can be accurately determined by measurement of the beat frequency against the iodine-stabilized helium–neon laser at 633 nm. A 1.3-THz signal can be measured directly with a point-contact metal–insulator–metal diode.[24] Alternatively, a comb of frequencies that span more than 1.3 THz may be generated by driving an electro-optic phase modulator installed inside a Fabry–Perot cavity,[25] where both the rf and laser frequencies coincide with resonant frequencies of the cavity. This system will provide a beat frequency that can be measured with a conventional high-frequency optical detector.

A systematic study of the frequency shifts of an iodine-stabilized Nd:YAG laser, e.g., caused by pressure, laser power, or modulation frequency, may be required to establish this source as a frequency reference. Compared with the 633-nm helium–neon laser locked to an intracavity iodine cell, which has to be maintained at a higher temperature because of the low population of the $v'' = 5$ level, there is a potential for reduced power and pressure-induced line shifts.[3] The reproducibility may also be limited by offsets owing to residual amplitude modulation at the modulation frequency of the electro-optic modulator. This effect is usually caused by polarization rotation in the electro-optic birefringent crystal, followed by polarization-dependent transmission through the optical elements. In our system we have manually adjusted the orientation of the electro-optic modulator with respect to the polarization of the probe beam to minimize the residual amplitude modulation. However, for measurements of the absolute frequency of the iodine transitions, a servo control that actively suppresses the amplitude modulation may be required.[26]

5. SUMMARY

We have measured the spectra and determined the hyperfine constants of several rovibrational transitions near 532 nm. These transitions occur between the lowest vibrational level in the ground X state and the vibrational levels 32–36 in the B state. The determination of the hyperfine constants provides additional information on the dependence of the hyperfine constants on the vibrational level. We have also precisely measured the frequency spacing between hyperfine components belonging to the different rovibrational transitions near 532 nm, thereby creating an absolute high-resolution frequency reference scale that matches the tuning range of doubled Nd:YAG lasers.

The iodine-locked Nd:YAG laser offers several important advantages with respect to other frequency references in the visible: higher power and a stronger iodine transition compared with the red helium–neon lasers and narrower linewidth, smaller size, and higher electrical efficiency with respect to the argon-ion lasers. If the absolute frequency of the lines studied in this paper were measured to a higher accuracy, then this all-solid-state laser could become an attractive optical-frequency reference and a new optical length standard for the definition of the meter.

ACKNOWLEDGMENTS

Ady Arie thanks A. L. Schawlow and M. D. Levenson for helpful discussions and the financial support of the Fulbright and Wolfson Fellowships. We thank Tim Day of New Focus for providing the high-frequency detector used in this research. This work was funded by National Science Foundation grant PHY-9215157 and by the Nippon Telegraph and Telephone Corporation.

*Present address, Faculty of Engineering, Tel Aviv University, Ramat Aviv, Tel Aviv 69978, Israel.

Note added in proof: Measurements of several iodine lines by use of a pulsed, injection-seeded and frequency-doubled ND:YAG laser were reported recently.[27]

REFERENCES AND NOTES

1. S. Gerstenkorn and P. Luc, *Atlas Du Spectre D'Absorption de la Molecule D'Iode* (Editions du CNRS, Paris, 1978).
2. S. Gerstenkorn and P. Luc, "Description of the absorption spectrum of iodine recorded by means of Fourier transform spectroscopy: the (B–X) system," J. Phys. (Paris) **46,** 867–881 (1985).
3. A. Brillet and P. Cerez, "Laser frequency stabilization by saturated absorption," J. Phys. (Paris) **42,** 73–82 (1981).
4. "Documents concerning the new definition of the metre," Metrologia **19,** 163 (1984).
5. S. V. Kruzhalov, V. A. Parfenov, L. N. Pakhomov, and V. Yu. Petrun'kin, "Hyperfine structure of $^{127}I_2$ absorption lines coinciding with the second harmonic frequency of a YAG:Nd laser," Opt. Spectrosc. (USSR) **59,** 414–416 (1985); S. V. Kruzhalov, V. A. Parfenov, L. N. Pakhomov, and V. Yu. Petrun'kin, "Frequency stabilization of a Nd:YAG laser by means of $^{127}I_2$ absorption lines," Sov. Tech. Phys. Lett. **11,** 111–112 (1985).
6. P. Esherick and A. Owyoung, "Polarization feedback stabilization of an injection-seeded Nd:YAG laser for spectroscopic applications," J. Opt. Soc. Am. B **4,** 41–47 (1987).
7. A. Arie, S. Schiller, E. K. Gustafson, and R. L. Byer, "Abso-

lute frequency stabilization of diode-laser-pumped Nd:YAG lasers to hyperfine transitions in molecular iodine," Opt. Lett. **17,** 1204–1206 (1992).
8. J. J. Snyder, R. K. Raj, D. Bloch, and M. Ducloy, "High sensitivity nonlinear spectroscopy using a frequency-offset pump," Opt. Lett. **5,** 163–165 (1980).
9. Opthos Instruments, Inc., 17805 Caddy Drive, Rockville, Md. 20855.
10. The calibrated iodine cell and the beat-frequency results against a reference helium–neon laser were provided by J. M. Chartier, Bureau International des Poids et Mesures, Pavillon de Breteuil, Sèvres Cedex, France.
11. M. Glaser, "An improved He–Ne laser at $\lambda = 612$ nm stabilized by means of an external absorption cell," Metrologia **23,** 45–53 (1986).
12. S. Gerstenkorn and P. Luc, "Absolute iodine (I_2) standards measured by means of Fourier transform spectroscopy," Rev. Phys. Appl. **14,** 791–794 (1979).
13. H. J. Foth and F. Spieweck, "Hyperfine structure of the $R(98)58$–1 line of $^{127}I_2$ at 514.5 nm," Chem. Phys. Lett. **65,** 347–352 (1979).
14. $eQq'' = -2452.5837$ MHz, $C'' = 3.162$ kHz, $a'' = 3.66$ kHz, $d'' = 1.58$ kHz; see A. Yokozeki and J. S. Munter, "Laser fluorescence state selected and detected molecular beam magnetic resonance in I_2," J. Chem. Phys. **72,** 3796–3804 (1980).
15. P. R. Bevington, *Data Reduction and Error Analysis for Physicists* (McGraw Hill, New York, 1969).
16. Ch. J. Bordé, G. Camy, B. Decomps, J. P. Descoubes, and J. Vigne, "High precision saturation spectroscopy of $^{127}I_2$ with argon lasers at 5145 Å and 5017 Å—main resonances," J. Phys. (Paris) **42,** 1393–1411 (1981).
17. M. D. Levenson and A. L. Schawlow, "Hyperfine interactions in molecular iodine," Phys. Rev. A **6,** 10–20 (1972).
18. M. Glaser, "Identification of hyperfine structure components of the iodine molecule at 640 nm wavelength," Opt. Commun. **5,** 335–342 (1985).
19. R. F. Barrow and K. K. Yee, "*B*–*X* system of $^{127}I_2$: rotational analysis and long range potential in the *B* state," J. Chem. Soc. Faraday Trans. 2 **69,** 684–700 (1972).
20. D. C. Gerstenberger, G. E. Tye, and R. W. Wallace, "Efficient second-harmonic conversion of cw single-frequency Nd:YAG laser light by frequency locking to a monolithic ring doubler," Opt. Lett. **16,** 992–994 (1991).
21. D. A. Jennings, C. R. Pollock, F. R. Petersen, R. E. Drullinger, K. M. Evenson, J. S. Wells, J. L. Hall, and H. P. Layer, "Direct frequency measurement of the I_2-stabilized He–Ne 473-THz (633 nm) laser," Opt. Lett. **8,** 136–138 (1983). After the submission of this paper a new measurement of the 633-nm iodine-stabilized helium–neon laser frequency with 10^{-11} accuracy was published: O. Acef, J. J. Zondy, M. Abed, D. G. Rovera, A. H. Gerard, A. Clarion, Ph. Laurent, Y. Millerioux, and P. Juncar, "A CO_2 to visible optical frequency chain: accurate measurement of the 473 THz HeNe/I_2 laser," Opt. Commun. **97,** 29–34 (1993).
22. H. R. Telle, D. Meschede, and T. W. Hänsch, "Realization of a new concept for visible frequency division: phase locking of harmonic and sum frequencies," Opt. Lett. **15,** 532–534 (1990).
23. N. C. Wong, "Optical frequency counting from the UV to the near IR," Opt. Lett. **17,** 1155–1157 (1992).
24. R. E. Drullinger, K. M. Evenson, D. A. Jennings, F. R. Petersen, J. C. Bergquist, L. Burkins, and H. U. Daniel, "A 2.5 THz frequency difference measurement in the visible using metal-insulator metal diodes," Appl. Phys. Lett. **42,** 137–138 (1983).
25. D. W. Sesko and C. E. Wieman, "High-frequency Fabry–Perot phase modulator," Appl. Opt. **26,** 1693–1695 (1987); M. Kourogi, K. Nakagawa, and M. Ohtsu, "A wideband optical frequency comb generator for a highly accurate laser frequency measurement," presented at the International Quantum Electronics Conference, Vienna, Austria, 1992, paper TuM5.
26. N. C. Wong and J. L. Hall, "Servo control of amplitude modulation in frequency-modulation spectroscopy: demonstration of shot-noise-limited detection," J. Opt. Soc. Am. B **2,** 1527–1533 (1985).
27. J. A. Harrison, M. Zahedi, and J. W. Nibler, "Use of seeded Nd:YAG lasers for high-resolution spectroscopy," Opt. Lett. **18,** 149–151 (1993).